JOURNAL OF CATALYSIS 108, 233–246 (1987)

Infrared and Mössbauer Spectroscopy Studies of the Interaction of NO with Iron-Exchanged Zeolites

LUIS M. APARICIO,* W. KEITH HALL,[1] SHIU-MIN FANG,[1] MARIA A. ULLA,† WILLIAM S. MILLMAN,† AND J. A. DUMESIC*,[2]

*Department of Chemical Engineering, University of Wisconsin, Madison, Wisconsin 53706; and †The Laboratory of Surface Studies, Department of Chemistry, University of Wisconsin, Milwaukee, Wisconsin 53201

Received April 27, 1987; revised June 23, 1987

Nitric oxide adsorption on iron-exchanged, silicon-substituted Y-zeolite, iron-exchanged mordenite, and iron-exchanged ZSM-5 has been studied by both infrared and Mössbauer spectroscopies. In addition, the catalytic activities of these zeolites for nitrous oxide decomposition have been determined. The results show that NO adsorption is qualitatively the same for all the zeolites. However, the framework differences and the locations of the exchangeable cations control the relative concentrations of the various nitrosyl species formed upon adsorption. Zeolites that have a large fraction of the iron in accessible, low-coordination sites form predominantly mononitrosyls. Those zeolites that have a large fraction of iron in inaccessible, high-coordination sites form predominantly dinitrosyls and form them slowly. Measurements of catalytic activity and NO adsorption capacities correlate well with the relative accessibilities of the cations to reactant molecules. This indicates that the active sites for reaction are associated with those sites which form mononitrosyl species with NO. Thus, in Y-zeolite differences in activities can be accounted for by the changes in cation siting brought about by changes in the framework aluminum content.

INTRODUCTION

The interaction of NO with first row transition metals exchanged into zeolites has been studied extensively using infrared and EPR spectroscopies (*1–10*). In spite of this, no clear picture of how NO molecules interact with the cations has emerged. Some authors have interpreted their results in terms of cationic nitrosyl ligands (*2, 5, 8*). Others have proposed models in which the nitrosyl ligands are neutral and the oxidation state of the cations remains unchanged after adsorption (*1, 3, 4, 6, 7, 9*). In some cases (e.g., Cr(II)–Y, Cr(III)–Y, and Co(II)–Y), the infrared spectrum of adsorbed NO displays a pair of bands attributable to a dinitrosyl species (*1, 3, 6, 7*). In other cases (e.g., Ni(II)–Y and Cu(I)–Y), only one band attributable to a mononitrosyl species forms (*2, 9, 10*). In the infrared spectrum of NO adsorbed on Fe(II)–Y, both dinitrosyl and mononitrosyl species are observed, and relative concentrations of these species change with time after adsorption (*4*).

In an earlier study of the adsorption of NO on Fe–Y, a comparison was made between infrared and Mössbauer spectroscopic results. Whereas bands corresponding to both mono- and dinitrosyl species appeared in the infrared spectra, only one iron–nitrosyl species was detected by Mössbauer spectroscopy. Mössbauer spectroscopy may not have been capable of detecting more than one iron–nitrosyl species because of the large fraction of iron cations that remained inaccessible to NO. In conventional Fe–Y, most of the iron cations reside in site I, inaccessible to many

[1] Present address: University of Pittsburgh, Department of Chemistry, Pittsburgh, PA 15260.

[2] To whom all correspondence should be addressed.

0021-9517/87 $3.00

adsorbent gas molecules. Since the quadrupole doublet of cations at this site dominates the spectrum, other doublets arising from cations at different sites, where interaction with adsorbent molecules can occur, are difficult to observe.

Hence, the infrared and Mössbauer spectroscopic studies were recently extended to iron-exchanged zeolites having a larger fraction of their iron cations in sites that are accessible to NO. Spectra were collected for silicon-substituted Fe–Y, iron-exchanged mordenite (Fe–M), and iron-exchanged ZSM-5 (Fe–ZSM-5). Silicon-substituted Fe–Y was recently found by Mössbauer spectroscopy to have a large fraction of cations at sites I′, II′, and/or II; in addition, it was found to have a higher catalytic activity for the decomposition of N_2O into its elements than conventional Fe–Y (*11*). Like silicon-substituted Fe–Y, Fe–M is believed to have most of its iron cations in accessible sites (*12*). The Fe–M is interesting because, despite its smaller pore system, it has been found to exhibit higher turnover frequencies for the N_2O decomposition reaction and for the oxidation of CO with O_2, NO, and N_2O than conventional Fe–Y (*13, 14*). Furthermore, gravimetric and volumetric redox studies have shown that CO can react with the structural hydroxyl groups in Fe–M in a manner similar to that of the water–gas-shift reaction; the same behavior is not observed for Fe–Y (*15*). Although little is known about ion-exchange sites in Fe–ZSM-5, this zeolite was included in the study to investigate the behavior of zeolites having a higher silicon-to-aluminum ratio than either Fe–Y or Fe–M.

In addition to the infrared and Mössbauer spectroscopic studies, NO uptakes and catalytic activities for N_2O decomposition were measured for these same zeolite samples. The results obtained reinforced conclusions reached in previous studies of Fe–Y, and contributed new knowledge about NO adsorption in zeolites exchanged with iron and other transition metals. Since NO is a pollutant present in combustion gases, such knowledge could be useful in the development of zeolite-based exhaust gas catalysts.

EXPERIMENTAL

The starting materials for the Fe–M and Fe–Y zeolites were Linde sodium mordenite (LZ-M5, lot 8350-5), and Linde sodium Y-zeolite (SK-40, lot 1280-133). Sodium ZSM-5 was prepared by the method of Flanigen (*16*), and its crystallinity was checked by X-ray diffraction using methods discussed previously (*11*). The silicon-substituted Y-zeolites were prepared using the method of Skeels and Breck (*17*) where $(NH_4)_2SiF_6$ is reacted with an aqueous suspension of NH_4Na–Y. The measured crystallinities of these samples have been reported elsewhere (*11*). All the Fe zeolites were prepared by exchange of the sodium form of the zeolites as described previously (*4, 11*). The unit cell compositions, iron loadings, and silicon-to-aluminum (Si/Al) ratios of the final catalysts are reported in Table 1 and are based on analytical data provided by Galbraith Laboratories.

A conventional BET system was used to measure the NO uptakes. Approximately 0.2 g of catalyst was placed in an adsorption cell and evacuated at temperatures which were increased in 50 K stages from room temperature to 745 K; 30 min was allowed for each step. The catalysts were then treated in flowing O_2 (60 cc/min) for 1 h, reduced in CO for 1 h, and evacuated for 30 min. The temperature was then lowered to room temperature and the samples were exposed to 1400 Pa of NO for 30 min, unless otherwise stated.

A Nicolet MX-1 Fourier transform spectrometer was used to obtain infrared spectra. A vacuum-tight IR cell with KBr windows having a self-contained furnace was used for all IR experiments (*4*). Infrared samples were prepared as self-supporting platelets with a thickness of 4 to 10 mg/cm^2. The procedure used to pretreat the samples

TABLE 1

Unit Cell Compositions of Samples Studied

	Unit cell compositions	Si/Al ratio	Fe Loading ($\times 10^{-20}$ Fe/g)	Adsorption capacity 77 K (cc STP/g)
(Fe–Y)	$H_{5.3}Na_{22.6}Fe_{13.6}(AlO_2)_{55.0}(SiO_2)_{137.0}$	2.49	6.39	180
(Fe–Y)	$H_{3.5}Na_{12.0}Fe_{9.6}(AlO_2)_{34.1}(SiO_2)_{157.9}$	4.64	4.53	183
(Fe–Y)	$H_{8.6}Na_{5.6}Fe_{6.3}(AlO_2)_{26.8}(SiO_2)_{165.4}$	6.17	2.99	161
(Fe–Y)	$H_{2.0}Na_{4.4}Fe_{6.5}(AlO_2)_{19.4}(SiO_2)_{172.6}$	8.88	2.94	171
(Fe–M)	$H_{0.3}Na_{3.8}Fe_{1.4}(AlO_2)_{6.8}(SiO_2)_{41.2}$	6.06	2.67	100
(Fe–ZSM5)	$H_{1.7}Na_{2.7}Fe_{0.4}(AlO_2)_{5.2}(SiO_2)_{90.8}$	17.50	0.40	NA
(Fe–ZSM5)[a]	$H_{2.6}Na_{2.0}Fe_{0.3}(AlO_2)_{5.2}(SiO_2)_{90.8}$	17.50	0.30	NA

[a] This sample was used only for the Mössbauer spectra of Fig. 11. The iron in this zeolite was enriched in ^{57}Fe.

was the same as that used in the NO uptake experiments. It included one evacuation step while heating to 770 K in stages, O_2 pretreatment, reduction (H_2 or CO), and finally evacuation prior to decreasing the temperature to ambient for NO adsorption.

The details of the Mössbauer spectroscopy and measurement of catalytic activity experiments, as well as the gas purification procedures and X-ray crystallinity measurements, have been described elsewhere (*11*).

RESULTS

Infrared Spectroscopy

Infrared spectra of NO adsorbed on the iron-exchanged zeolites used in this study are shown in Fig. 1. The spectra were collected at room temperature after exposing reduced samples to 400 Pa of NO for 20 s, followed by a 30-min evacuation. This procedure was followed to minimize the migration of iron cations from inaccessible to accessible sites observed previously in the presence of NO (*4*). The spectra of the different samples all exhibit a dominant band centered near 1880 cm^{-1}. This band was previously assigned to an iron mononitrosyl species formed by the interaction of NO with immediately accessible iron (*4*). Thus, the results show that all the zeolites reported here have a similar and predominant mononitrosyl species which appears immediately after exposure to NO. Some of the spectra, particularly the spectrum of the Fe–Y sample with an Si/Al ratio of 2.5, exhibit smaller bands centered at about 1918, 1845, 1815, and 1765 cm^{-1}. These

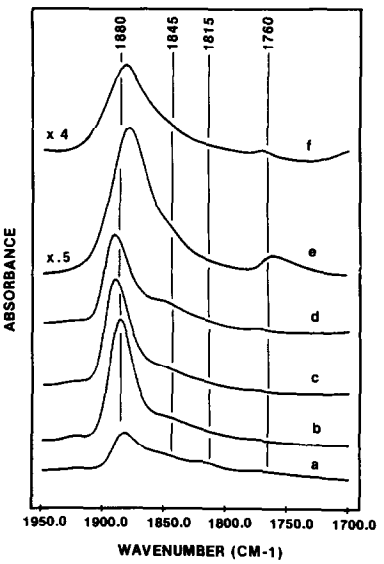

FIG. 1. Infrared spectra after exposure to 400 Pa of NO for 20 s followed by 30 min evacuation. (a) Fe–Y (Si/Al = 2.49), (b) Fe–Y (Si/Al = 4.64), (c) Fe–Y (Si/Al = 6.17), (d) Fe–Y (Si/Al = 8.88), (e) Fe–M (Si/Al = 6.06), (f) Fe–ZSM-5 (Si/Al = 17.5).

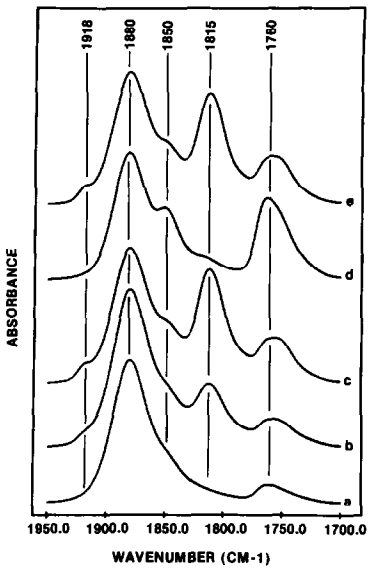

FIG. 2. Infrared spectra of Fe–M following different treatments; (a) 400 Pa of NO for 20 s and evacuated, (b) 400 Pa for 10 min, (c) 400 Pa for 18 h, (d) following 1 h evacuation, (e) after reexposure to 400 Pa of NO for 10 min.

bands were previously assigned to mononitrosyls (1845 and 1765 cm^{-1}) and a dinitrosyl species (1918 and 1815 cm^{-1}). Their relative intensities vary with the particular zeolite sample and likely reflect the differences in cation siting between zeolites.

The changes in intensities of the various bands in Fe–M with time were also investigated. The results are shown in Fig. 2. After the spectrum shown in Figs. 1e and 2a was obtained, the Fe–M sample was exposed to 400 Pa of NO for 10 min and spectrum 2b was collected. The sample was kept under NO at room temperature for 18 h, after which spectrum 2c was collected. Subsequently, the sample was evacuated at room temperature for 1 h and spectrum 2d was collected. Thereafter, the sample was reexposed to 400 Pa of NO and spectrum 2e collected. These results are similar to those obtained with Fe–Y zeolite (*4*). The spectra show two bands assigned to mononitrosyl species (1880 and 1760 cm^{-1}) appearing immediately after exposure to NO, with a shoulder appearing at ca. 1850 cm^{-1}. After reexposure for 10 min, bands at 1815 and 1918 cm^{-1} appear and the bands that were previously present increase somewhat in intensity. The bands at 1918 and 1815 cm^{-1} have been assigned to the two stretching modes of a dinitrosyl species that forms slowly as cations migrate to sites of low coordination where they are sufficiently accessible to form the dinitrosyl species (*4*). Upon evacuation, this dinitrosyl species converts to a mononitrosyl species, through the loss of one NO ligand, giving rise to a band at 1760 cm^{-1} (*4*). This explains the decrease in the 1918- and 1815-cm^{-1} bands and the increase in the 1760-cm^{-1} band during this step. In addition to the band at 1760 cm^{-1}, the band at 1850 cm^{-1} also increased in intensity during evacuation. When the sample was reexposed to NO after evacuation, the bands associated with the dinitrosyl species increased in intensity, accompanied by a decrease in intensity of the bands at 1760 and 1850 cm^{-1}. These results show that in Fe–M, as in Fe–Y, some iron cations are sufficiently accessible to form mononitrosyl species immediately upon contact with NO. Others form dinitrosyl species after having migrated from inaccessible sites to more accessible sites. As in the case of Fe–Y, the dinitrosyl species in Fe–M can be converted to a mononitrosyl species by room temperature evacuation. In contrast to Fe–Y, the mononitrosyl species at 1760 cm^{-1} forms immediately upon contact of Fe–M with NO. The changes seen in the 1850-cm^{-1} band with Fe–M are not detected in Fe–Y.

To study the effects of the Si/Al ratio on the adsorption of NO, the experiments just described for Fe–M were also carried out with three Fe–Y samples having different Si/Al ratios. The results are shown in Figs. 3, 4, and 5. The samples were conventional Fe–Y (Si/Al = 2.49) and silicon-substituted Fe–Y (Si/Al = 6.17 and 8.88). Immediately upon exposure to NO a strong band appears at 1880 cm^{-1} in the spectra of all

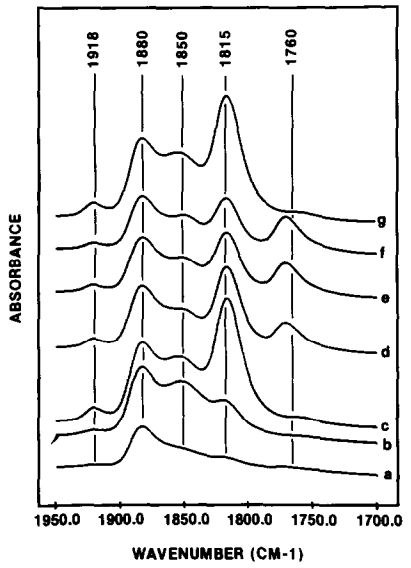

FIG. 3. Infrared spectra of Fe–Y (Si/Al = 2.49) after different treatments; (a) 400 Pa of NO for 20 s and evacuated, (b) 400 Pa for 10 min, (c) 400 Pa for 16 h, (d) after 20 min evacuation, (e) after 40 min evacuation, (f) after 1 h evacuation, (g) after reexposure to 400 Pa of NO for 10 min.

samples. With the lower Si/Al ratio samples, no other bands are readily distinguishable, although there is an indication that there may be very small contributions to the spectra from the 1850-cm^{-1} band and possibly the 1815- and 1918-cm^{-1} bands in spectrum 4a. In the case of the sample with an Si/Al ratio of 8.88, bands at 1918, 1880, 1850, and 1815 cm^{-1} are clearly present. Additionally, this sample has a low-frequency mononitrosyl band (ca. 1760 cm^{-1}), similar to that observed with Fe–M. Upon exposure to NO for a prolonged period of time, the dinitrosyl bands at 1815 and 1918 cm^{-1} grow as a function of time along with the mononitrosyl band at 1850 cm^{-1} in all samples. The changes in this latter band were similar to those observed with Fe–M. Interestingly, the 1760-cm^{-1}

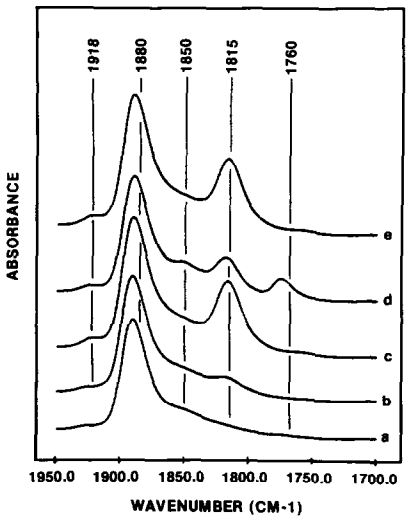

FIG. 4. Infrared spectra of Fe–Y (Si/Al = 6.17) after different treatments; (a) 400 Pa of NO for 20 s and evacuated, (b) 400 Pa for 10 min, (c) 400 Pa for 24 h, (d) following 1 h evacuation, (e) after reexposure to 400 Pa of NO for 10 min.

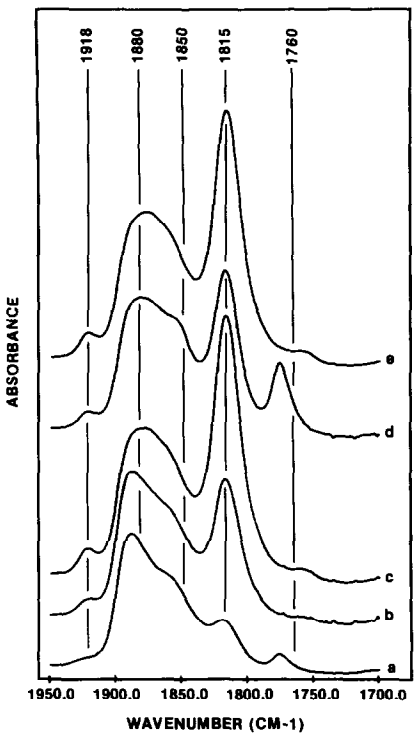

FIG. 5. Infrared spectra of Fe–Y (Si/Al = 8.88) after different treatments; (a) 400 Pa of NO for 20 s and evacuated, (b) 400 Pa for 10 min, (c) 400 Pa for 18 h, (d) following 1 h evacuation, (e) after reexposure to 400 Pa of NO for 1 min.

TABLE 2

NO Uptakes and Band Intensities

Zeolite	Si/Al ratio	NO band intensity[a]	Ambient NO uptake (μm/g)	NO/Fe (mol NO/mol Fe)
Fe–Y	2.49	1170	180	0.17
Fe–Y	4.64	1740	170	0.22
Fe–Y	6.17	1990	130	0.26
Fe–Y	8.88	2120	130	0.27
Fe–M	6.06	6700	310	0.70
Fe–ZSM5	17.50	4140	34	0.51

[a] Band intensities are normalized to a wafer density of 1×10^{18} Fe/cm^2.

band originally present in the sample with an Si/Al ratio of 8.88 disappeared upon exposure for a prolonged period of time. Evacuation of all three samples after prolonged exposure resulted in the growth of the mononitrosyl band at 1760 cm^{-1} together with a decrease in the dinitrosyl bands. With the exception of the sample with an Si/Al ratio of 8.88, only a very slight change was observed for the mononitrosyl band at 1850 cm^{-1} during this procedure. Upon reexposure to NO, the 1760-cm^{-1} band decreased in intensity while the dinitrosyl bands increased in intensity. The principal difference between the spectra shown in Figs. 3–5 is that the spectra of conventional Fe–Y (Fig. 3) and Fe–Y (Si/Al = 8.88) (Fig. 5) are dominated by the dinitrosyl species after prolonged exposure to NO whereas the spectrum of Fe–Y (Si/Al = 6.17) (Fig. 4) has the 1880-cm^{-1} band as the dominant peak.

NO Uptake and Catalytic Activity

The integrated intensities of the NO bands shown in Fig. 1 are listed in Table 2 (normalized to a platelet density of 1×10^{18} Fe/cm^2). In addition, measured NO uptakes and NO uptakes per iron loading are given. Changing from an Si/Al ratio of 2.49 to 8.88 in Fe–Y, the NO uptake decreases from 180 to 130 μmol/g. However, the Fe content decreases by a factor of 2. Hence, when the data are converted to molecules of NO per iron atom, it is found that the NO uptake increased from 0.17 to 0.27 molecules of NO per atom of iron. This result demonstrates that the iron becomes more accessible to the NO as the Si/Al ratio increases in Fe–Y. This reinforces the previous conclusion that silicon-substituted Fe–Y has a larger fraction of iron cations in sites accessible to adsorbent molecules than conventional Fe–Y (*11*). This effect is even more pronounced in the Fe–M and Fe–ZSM-5 samples. The NO uptakes per iron measured for Fe–M and Fe–ZSM-5 were four and three times greater than those of conventional Fe–Y, respectively.

The relative catalytic activities for the decomposition of N_2O on these zeolites agreed well with the above observations. The turnover frequency (TOF) for the reaction at 800 K increased with the Si/Al ratio for Fe–Y, and was even higher for Fe–M and Fe–ZSM-5. The correlation of TOF and NO uptake per iron atom is shown in Fig. 6. The data demonstrate the catalytic effectiveness of the iron capable of coordinating NO. The overall infrared band area per iron atom was found to vary fairly linearly with the NO uptakes on a per iron basis. This result is shown in Fig. 7.

Mössbauer Spectroscopy

The Mössbauer spectroscopy studies probing the interaction of NO with the zeolites were limited to the Fe–Y samples and Fe–M since the amount of iron in Fe–ZSM-5 was too low. The zeolites were reduced in flowing H_2 at 700 K for ca. 5 h, cooled to room temperature, and subsequently evacuated. After this pretreatment, they were exposed to 700 Pa of NO for 15 s, the cell was evacuated, and Mössbauer spectra were collected with the samples *in vacuo*. This procedure was followed to reproduce the conditions under which the infrared spectra shown in Fig. 1 were obtained. Thereafter, the zeolites were reexposed to 700 Pa of NO, and Mössbauer spectra were collected in NO starting 1 h after reexposure. This was done to observe the appearance of the dinitrosyl species

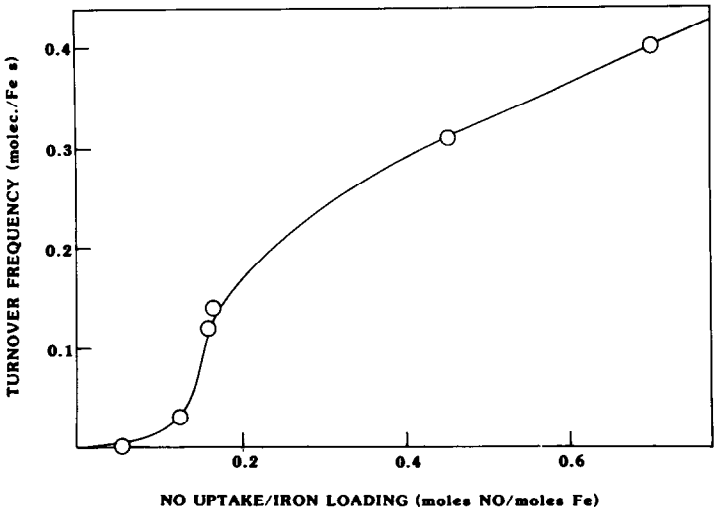

FIG. 6. Correlation between turnover frequency and NO uptake per atom of iron.

that had been seen in the IR spectra. After the spectra in the presence of NO were collected, spectra were collected with the samples *in vacuo*. These spectra were designed to investigate the conversion of the dinitrosyl species into mononitrosyl species.

Figures 8–10 show the spectra collected for conventional Fe–Y, silicon-substituted Fe–Y (Si/Al = 8.88) and Fe–M. The results obtained after computer fitting the spectra of Figs. 8–10 are summarized in Table 3. Before adsorption of NO, all three samples exhibited two ferrous quadrupole doublets, one with a larger isomer shift and quadrupole splitting. The adsorption of NO on Fe–Y initially formed a doublet that was superimposed on the ferrous doublet with the larger isomer shift and quadrupole splitting. Although this is not clear in the spec-

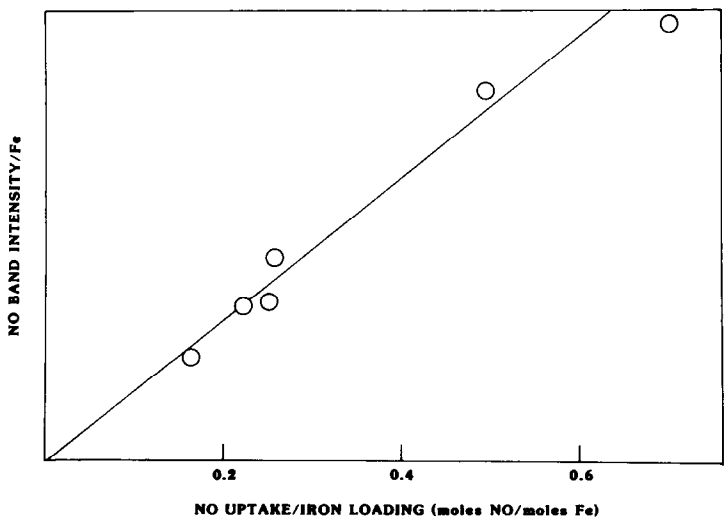

FIG. 7. Correlation between overall NO band intensities and NO uptakes.

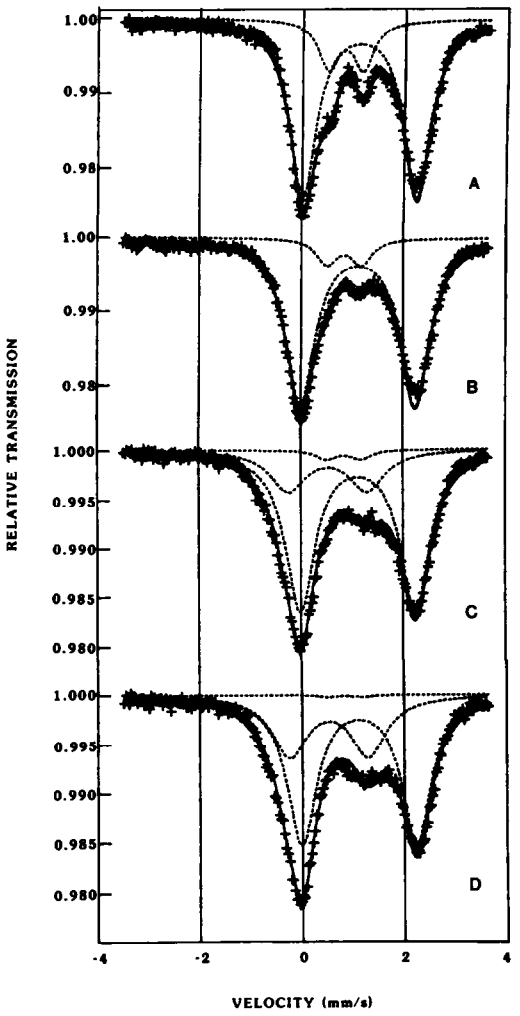

FIG. 8. Mössbauer spectra of Fe–Y (Si/Al = 2.49) after different treatments; (A) reduction in H_2 for 5 h, (B) 700 Pa of NO for 15 s and evacuated, (C) 700 pa of NO for 20 h, (D) ambient evacuation for 1 h.

tra of conventional Fe–Y, it is readily seen in the spectra of silicon-substituted Fe–Y. This result is very similar to the results previously obtained for adsorption of both CO and H_2O on an identical silicon-substituted sample (*11*). It shows that adsorbed NO initially increases the coordination of the ferrous cations at sites I′, II′, and/or II without changing the oxidation state of the iron. The results obtained for Fe–M were similar to those obtained for Fe–Y, with the exception that the iron mononitrosyl doublet could be resolved from the ferrous doublets.

When the zeolites were exposed to NO for a prolonged period of time, a second doublet appeared which had an isomer shift between the values characteristic of high-spin Fe^{2+} and Fe^{3+}. This doublet has been observed in previous studies of the interaction of NO with conventional Fe–Y (*4*).

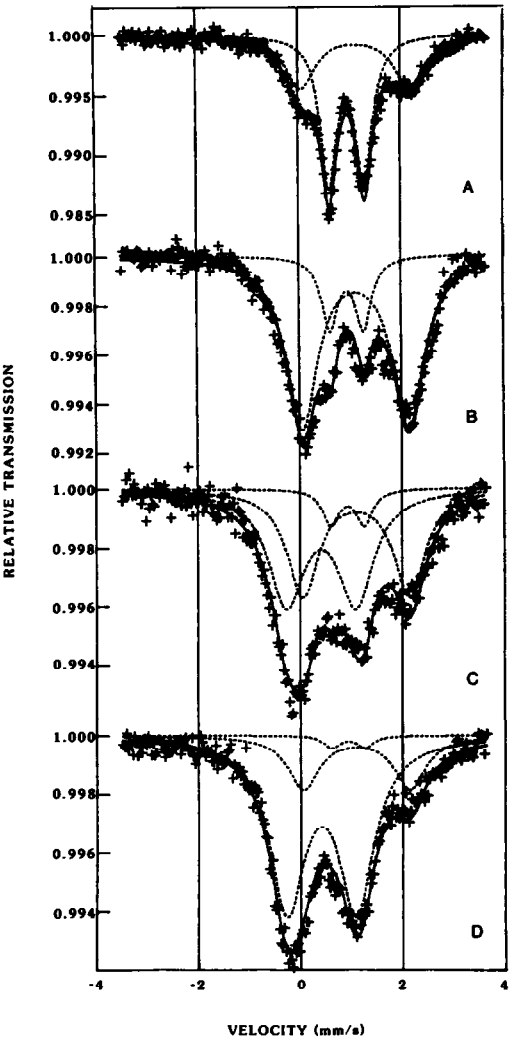

FIG. 9. Mössbauer spectra of Fe–Y (Si/Al = 8.88) after different treatments; (A) reduction in H_2 for 5 h, (B) 700 Pa of NO for 15 s and evacuated, (C) 700 Pa of NO for 20 h, (D) ambient evacuation for 1 h.

TABLE 3

Mössbauer Spectroscopy Spectral Areas of Doublets in Figs. 8–10[a]

Doublet	Pretreatment				Isomer Shift (mm/s)	Quadrupole splitting (mm/s)
	Hydrogen reduction	NO, 15 s, evacuation	NO many hours	Subsequent evacuation		
			Fe–Y (Si/Al = 2.49)			
Outer doublet + Fe–NO doublet No.1	4.62	4.83	3.86	3.55	1.12–1.13	2.24–2.25
Inner doublet	0.96	0.53	0.13	0.04	0.85	0.68
Fe–NO doublet No.2	—	—	1.06	1.57	0.53	1.54
			Fe–Y (Si/Al = 8.88)			
Outer doublet + Fe–NO doublet No.1	0.98	1.89	0.98	0.49	1.10–1.12	2.09–2.13
Inner doublet	1.47	0.35	0.14	0.05	0.94–0.96	0.66–0.69
Fe–NO doublet No.2	—	—	1.00	1.50	0.41	1.36
			Fe–M (Si/Al = 6.06)			
Outer doublet	1.73	1.54	0.72	0.37	1.06	2.20
Inner doublet	0.71	0.16	0.04	0.03	0.81	1.05
Fe–NO doublet No.1	—	0.58	0.51	0.55	0.57	1.58
Fe–NO doublet No.2	—	—	1.31	1.55	0.34	1.42

[a] Spectral areas given in percentage times millimeters per second.

Since it appeared only after long NO exposures, it was assigned to an iron dinitrosyl species in agreement with the infrared results. The fact that this doublet has a lower isomer shift than the value characteristic of high-spin Fe^{2+} indicates that the two NO ligands may change either the oxidation state of the spin state of the iron cations.

After the zeolites were evacuated, no new peaks appeared. Rather, the dinitrosyl doublet seemed to increase in intensity. During the same step, the IR spectra showed the conversion of the dinitrosyl species to a mononitrosyl species. That no change other than a small increase in the contribution of the doublet associated with the dinitrosyl occurs in the Mössbauer spectra can be taken as evidence that the mononitrosyl species produced in this step is at the same site as the dinitrosyl species. As a result, the mononitrosyl species may be expected to have similar Mössbauer parameters. This would indicate that this mononitrosyl species (like the dinitrosyl species) may also involve iron in a different oxidation state or spin state than the exchanged ferrous cations. In this sense, this mononitrosyl species would contrast with the mononitrosyl species formed initially.

Mössbauer spectra of iron-exchanged ZSM-5 are shown in Fig. 11. Although the iron in this sample was enriched in ^{57}Fe, the loading was too low to obtain a sufficiently high signal-to-noise ratio in the spectra to allow NO adsorption studies. The spectra shown were collected after oxidation with O_2 at 700 K for 5 h, after reduction with H_2 at 700 K for 5 h, and after exposure of the reduced sample to 10^5 Pa of CO. The spectrum collected after treatment with O_2 showed that most of the iron is Fe^{3+}. In the spectrum collected after reduction with H_2, a large fraction of the spectral area is composed of a ferrous doublet with a low isomer shift and quadrupole splitting. Such doublets have been assigned to ferrous cations in sites of low coordination and high accessibility (*11*). The spectrum, therefore,

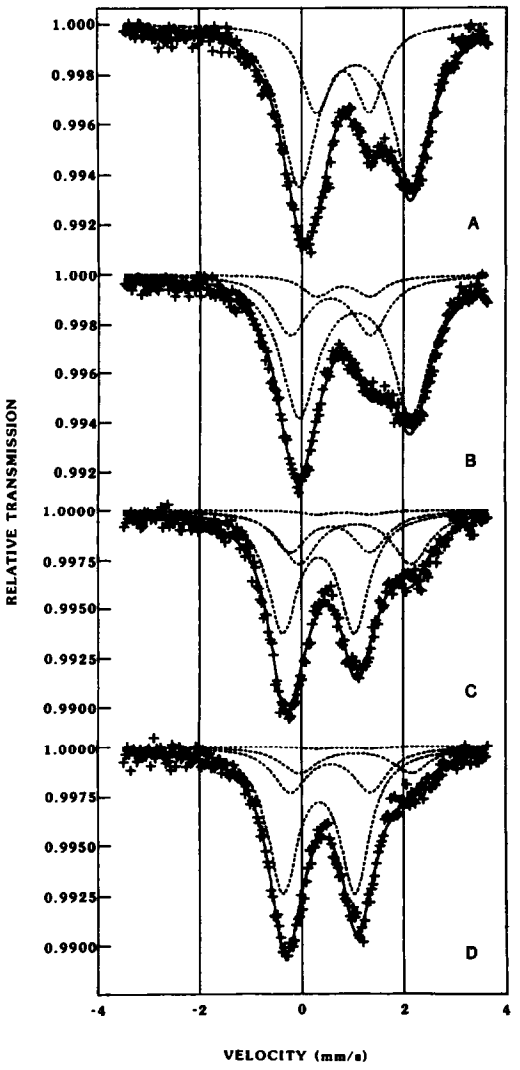

FIG. 10. Mössbauer spectra of Fe–M (Si/Al = 6.06) after different treatments; (A) reduction in H_2 for 5 h, (B) 700 Pa of NO for 15 s and evacuated, (C) 700 Pa of NO for 20 h, (D) ambient evacuation for 1 h.

indicated that Fe–ZSM-5, like Fe–M and silicon-substituted Fe–Y, has a large fraction of iron cations in sites that are accessible to reactant molecules. This was confirmed in the spectrum collected after exposure to CO. Carbon monoxide adsorbed on these iron cations, increasing their coordination and thus increasing the resulting quadrupole splitting.

DISCUSSION

Relationship between Infrared and Mössbauer Spectroscopies

The various infrared bands observed in this work are summarized in Table 4. Earlier work using NO adsorption, carried out on conventional Fe–Y, assigned the IR bands at 1918 and 1815 cm^{-1} to an iron dinitrosyl species at site III′, the 1880-cm^{-1} band to a sterically hindered mononitrosyl species at site II′, and the 1850-cm^{-1} band to a mononitrosyl species at site II. The mononitrosyl species at 1760 cm^{-1} was assigned to a species resulting from the desorption of one of the nitrosyl ligands from the site III′ dinitrosyl species (*4*). In

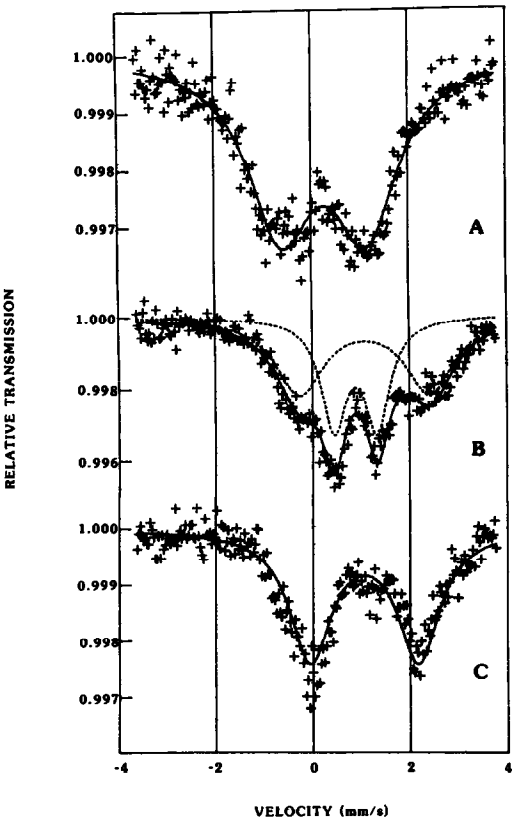

FIG. 11. Mössbauer spectra of Fe–ZSM-5 (Si/Al = 17.5) after different pretreatments: (A) after oxidation in oxygen for 5 h, (B) after reduction in hydrogen for 5 h, (C) after exposure of reduced sample to 10^5 Pa of CO.

TABLE 4

Summary of Observed Changes in IR Spectral Intensities

Band (cm^{-1})	Species	Treatment			
		NO 20 s, evacuate	NO many hours	Ambient evacuation	Reexposure
		Fe–Y (Si/Al = 2.49)			
1918, 1815	Dinitrosyl	Weak	Increases	Decreases	Grows back
1882	Mononitrosyl	Dominant	Unchanged	Little change	—
1850	Mononitrosyl	Present	Little change	Little change	—
1760	Mononitrosyl	Absent	Absent	Appears and Increases	Decreases
		Fe–Y (Si/Al = 6.17)			
1918, 1815	Dinitrosyl	Weak	Increases	Decreases	Increases
1882	Mononitrosyl	Dominant	Unchanged	Little change	—
1850	Mononitrosyl	Present	Little change	Little change	—
1760	Mononitrosyl	Absent	Absent	Appears and increases	Decreases
		Fe–M (Si/Al = 6.06)			
1918, 1815	Dinitrosyl	Absent	Increases	Decreases	Increases
1882	Mononitrosyl	Dominant	Unchanged	Little change	Little change
1850	Mononitrosyl	Present	Little change	Increases	Decreases
1760	Mononitrosyl	Present	Little change	Increases	Decreases

the previous work, the adsorption of NO on a reduced sample was found to generate immediately an iron mononitrosyl at sites of high accessibility. After prolonged NO exposure, a slow migration of Fe from site I to site III′ and the formation of a dinitrosyl species resulted. The time-dependent behavior of the dinitrosyl species that has been seen previously in conventional Fe–Y was also found in this work and appears to be a general characteristic of all the zeolites studied here. This includes not only the Y-zeolites having different Si/Al ratios, but also the mordenite and ZSM-5 samples.

Paralleling these results, the deconvoluted Mössbauer spectra show a conversion of the ferrous inner doublet (i.e., the doublet with the smaller quadrupole splitting) to a doublet overlapping the ferrous outer doublet immediately after NO exposure. After prolonged NO exposure, a new doublet with an isomer shift between the characteristic values of high-spin Fe^{2+} and Fe^{3+} appeared and grew with time. A contrast between the infrared and the Mössbauer spectroscopy results was seen upon room temperature evacuation after long exposure to NO. While the infrared spectra suggested the conversion of the dinitrosyl to a mononitrosyl species, the Mössbauer spectra showed an increase in the doublet with the isomer shift between the characteristic values of high-spin Fe^{2+} and Fe^{3+}. This apparent discrepancy can be explained by assuming that both the dinitrosyl species and the mononitrosyl species arising from the removal of one NO ligand from the dinitrosyl have similar Mössbauer parameters. If this is the case, the low isomer shift of the two species indicates that the iron involved in both of them is not high-spin Fe^{2+}, but either Fe^{3+} or low-spin Fe^{2+}.

Earlier, it was argued that the Fe–NO complex with an isomer shift between the characteristic values for high-spin Fe^{2+} and Fe^{3+} seen in the Mössbauer spectra was associated with a mononitrosyl species at sites II and/or II′ (*4*). However, Mössbauer spectra collected after exposure to NO for only a few seconds did not display this

doublet. Comparable spectra were unavailable in the earlier work. In this study, the doublet was not seen in the Mössbauer spectra until the samples had been exposed to NO for longer periods of time. Under the same conditions the infrared spectra showed a growth of the dinitrosyl species. Thus, one would expect the doublet to be associated with the dinitrosyl species, in contrast to the earlier interpretation.

Relationship with Catalytic Activity

The increase in turnover frequency TOF for the decomposition of N_2O as the Si/Al ratio increased was accompanied by a decrease in the Fe content brought about by a decrease in the exchange capacity of the zeolite. In conjunction with the increased TOF, there was an increase both in the intensity of the predominant mononitrosyl band on a per iron basis and in the amount of NO adsorbed per iron atom in the lattice. Thus, increasing the Si/Al ratio increased the ability of the iron cations to coordinate NO. However, because iron that is initially accessible to NO forms mononitrosyl species, the results imply that the active sites for N_2O decomposition are those on which not dinitrosyl but mononitrosyl species are formed. This stands in contrast to the mechanism by which the catalytic reduction of nitric oxide is believed to occur, i.e., two nitric oxide molecules coupling in the same cation to form nitrous oxide and an extra lattice oxygen atom (*18*). It is therefore possible that sites that are active for N_2O decomposition are not the same sites as those that are active for the reduction of NO.

Figure 6 shows the relationship between the TOF and the ability of the cations to coordinate NO. One would expect a linear relationship if the only effect of a higher Si/Al ratio were a greater accessibility of the cations to reactant molecules. The nonlinearity of the curve suggests that the more accessible sites are not only more effective in coordinating NO, but also have more favorable energetics for the decomposition of N_2O. Similar observations have been seen previously with these samples (*11*).

Nature of Dinitrosyl Species

The infrared spectral studies reported here all show the conversion of the dinitrosyl species to a mononitrosyl species upon evacuation at room temperature. This behavior has not only been observed in iron-exchanged zeolites, but also for NO adsorbed on iron supported on silica (*19*). In contrast, the dinitrosyl bands (1900 and 1780 cm^{-1}) for NO on Cr–Y (*1, 3*) and (1910 and 1820 cm^{-1}) for NO on Co–Y (*6, 7*) are not affected by evacuation at room temperature (*2, 6, 7*). Such results imply that dinitrosyl species on iron cations are relatively unstable compared with dinitrosyl species on other metals. One source of difference between NO on Fe cations and NO on other metals is associated with the dihedral angle of the dinitrosyl species. This angle can be calculated from the ratio of the intensities of the symmetric and antisymmetric stretching modes (*20*). Such an analysis yields dihedral angles of 105° for Cr–Y (*1*) and 122° for Co–Y. For Fe–Y, the angle is 145° (*4*). Similar dihedral angles can be deduced from the spectra of the dinitrosyls on Fe–M and Fe on silica. With such a large angle, dinitrosyl species in iron-exchanged zeolites and supported iron catalysts may form only on sites that protrude from the lattice (puckered). Such a process may take place on either site III or site III′ in Y-zeolite.

Such large angles between NO molecules in iron dinitrosyl species might also explain why such species do not form readily. Prior to NO exposure, Fe–Y and Fe–M are believed to have iron cations in sites where there is enough room for dinitrosyls to form. Nevertheless, dinitrosyls do not seem to form on cations occupying these sites. On site II in Fe–Y, steric hindrance from O_4 oxygens might impede the formation of a dinitrosyl species with such a large dihedral angle. On site IV in Fe–M (using the nomenclature from Ref. (*21*), steric

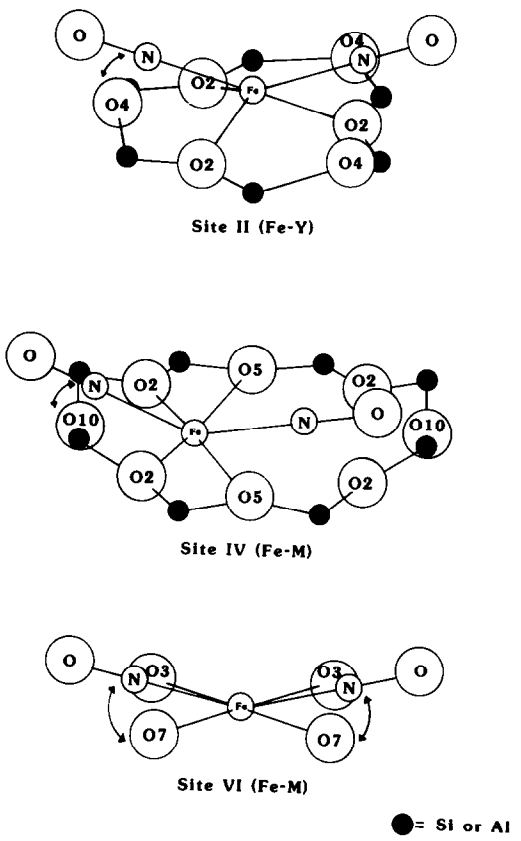

FIG. 12. Examples of steric hindrance impeding the formation of dinitrosyl species in Fe–Y and Fe–M prior to migration of cations. Arrows indicate probable interactions.

hindrance could come from the O_{10} oxygens. On site VI in Fe–M, the coordination of iron cations is almost planar, and steric hindrance could come from the oxygens to which the iron in bonded. These arguments are illustrated graphically in Fig. 12.

Cations for which dinitrosyl species have a smaller dihedral angle between the NO molecules would not encounter such steric difficulties and would explain why dinitrosyl species form readily on Cr–Y and Co–Y. Such dinitrosyl species could be at site II without encountering steric hindrance. This would also agree with the fact that Cr and Co cations supported on silica and alumina form dinitrosyl species more readily than does supported iron (*22–28*). On the other extreme would be cations like Ni and Cu. These cations form only mononitrosyl species either exchanged into zeolites (*2, 9, 10*) or supported on silica and alumina (*10, 29, 30*).

Although both mononitrosyl and dinitrosyl bands were observed for the zeolites studied, the relative concentrations of these species varied from one zeolite to another. The results show that zeolites with a large fraction of iron cations originally in accessible sites (e.g., silicon-substituted Fe–Y) form predominantly mononitrosyl species. Zeolites with a large fraction of iron cations in inaccessible sites (e.g., conventional Fe–Y) form predominantly dinitrosyl species, but only after a sufficient time to allow for cation migration. This is an indication that once NO is adsorbed it impedes any further migration of iron cations. Those cations that adsorb single NO molecules immediately after exposure become trapped and are unable to migrate to sites where dinitrosyl species can form. Only cations that are originally inaccessible to NO are able to migrate to such sites.

ACKNOWLEDGMENTS

The authors express their gratitude to the National Science Foundation for Grant CBT-8414622 which supported this work. One of us, W.S.M., also acknowledges the Union Oil Foundation for support.

REFERENCES

1. Pearce, J. R., Sherwood, D. E., Hall, M. B., and Lundsford, J. H., *J. Phys. Chem.* **84,** 3215 (1980).
2. Naccache, C., and Ben Taarit, Y., *J. Chem. Soc. Faraday Trans. 1* **69,** 1475 (1973).
3. Wichterlova, B., Tvaruzkova, Z., and Novakova, J., *J. Chem. Soc. Faraday Trans. 1* **79,** 1573 (1983).
4. Segawa, K., Chen, Y., Kubsh, J. E., Delgass, W. N., Dumesic, J. A., and Hall, W. K., *J. Catal.* **76,** 112 (1982).
5. Jermyn, J. W., Johnson, T. J., Vansant, E. F., and Lundsford, J. H., *J. Phys. Chem.* **77,** 2964 (1973).
6. Lundsford, J. H., Hutta, P. J., and Windhorst, K. A., *Inorg. Chem.* **17,** 607 (1978).
7. Windhorst, K. A., and Lundsford, J. H., *J. Amer. Chem. Soc.* **97,** 1407 (1975).
8. Kasai, P. H., Bishop, R. J., Jr., and McLeod, D., Jr., *J. Phys. Chem.* **82,** 279 (1978).

9. Chao, C., and Lundsford, J. H., *J. Phys. Chem.* **76,** 1546 (1972).
10. Lokhov, Y. A., and Davydov, A. A., *Kinet. Katal.* **20,** 1239 (1979).
11. Aparicio, L. M., Dumesic, J. A., Fang, S. M., Long, M. A., Ulla, M. A., Millman, W. S., and Hall, W. K., *J. Catal.* **104,** 381 (1987).
12. Garten, R. L., Gallard-Nechtstein, J., and Boudart, M., *Ind. Eng. Chem. Fundam.* **12,** 299 (1973).
13. Petunchi, J. O., and Hall, W. K., *J. Catal.* **78,** 327 (1982).
14. Leglise, J., Petunchi, J. O., and Hall, W. K., *J. Catal.* **86,** 392 (1984).
15. Fang, S. M., Petunchi, J. O., Leglise, J., Millman, W. S., and Hall, W. K., *J. Catal.* **93,** 6545 (1985).
16. Flanigen, E. M., and Grose, R. W., U.S. Patent #4,061,724 (1977).
17. Skeels, G. W., and Breck, D. W., "Proceedings of the Sixth Intern. Zeolite Confr." (D. Olson and A. Bisio, Eds.), p. 87. Butterworths, London, 1984.
18. Casewit, C. J., and Rappé, A. K., *J. Catal.* **89,** 250 (1984).
19. Yuen, S., Chen, Y., Kubsh, J. E., Dumesic, J. A., Topsøe, N., and Topsøe, H., *J. Phys. Chem.* **86,** 3022 (1982).
20. Beck, W., Melinkoff, A., and Stahl, R., *Chem. Ber.* **99,** 3721 (1966).
21. Mortier, W. J., *J. Phys. Chem.* **81,** 1334 (1977).
22. Kugler, E. L., Kokes, R. J., and Gryder, J. W., *J. Catal.* **36,** 142 (1975).
23. Zecchina, A., Garrone, E., Monterra, C., and Coluccia, S., *J. Phys. Chem.* **79,** 978 (1975).
24. Beck, D. D., and Lundsford, J. H., *J. Catal.* **68,** 121 (1981).
25. Ghiotto, G., Garrone, E., Della Betta, G., Fubini, B., and Giarnello, E., *J. Catal.* **80,** 249 (1983).
26. Peri, J. B., *J. Phys. Chem.* **78,** 588 (1974).
27. Rebenstorf, B., *Acta Chem. Scand. Ser. A* **31,** 208 (1977).
28. Topsøe, N., and Topsøe, H., *J. Catal.* **75,** 354 (1982).
29. Peri, J. B., *J. Catal.* **86,** 84 (1984).
30. London, J. W., and Bell, A. T., *J. Catal.* **31,** 32 (1973).